EFFECTS OF QUASI-PERIODIC PATTERN REGRESSION ON BOLD SIGNALS CORRELATED WITH INFRASLOW AND HIGHER FREQUENCY ELECTROPHYSIOLOGY

A Thesis
Presented to
The Academic Faculty

By

Hyun Koo Chung

In Partial Fulfillment
of the Requirements for the Degree
Master of Science in the
School of Biomedical Engineering

Georgia Institute of Technology and Emory University

December 2017

EFFECTS OF QUASI-PERIODIC PATTERN REGRESSION ON BOLD SIGNALS CORRELATED WITH INFRASLOW AND HIGHER FREQUENCY ELECTROPHYSIOLOGY

Approved by:

Dr. Shella D. Keilholz, Advisor
School of Biomedical Engineering
Georgia Institute of Technology and Emory University

Dr. Dieter Jaeger
School of Biology and Biomedical Engineering
Emory University

Dr. Eric Schumacher
School of Psychology
Georgia Institute of Technology

Date Approved: October 18, 2017

ACKNOWLEDGEMENTS

I would like to first thank my thesis advisor Dr. Shella Keilholz for the opportunity to conduct research in the Magnetic Imaging of Neural Dynamics (MIND) Lab. She was an excellent advisor who was always available and guided me throughout this journey. I am thankful for my current and former lab members Wenju Pan, Maysam Nezafati, Jacob Billings, Anzar Abbas, Sadia Shakil and Amrit Kashyap. Thankful for the discussions, insights, data collection, and research contributions to complete this project. My committee members Dr. Dieter Jaeger and Dr. Eric Schumacher provided valuable insight in improving the project. Furthermore, I am thankful for David Hong for helpful suggestions on the research project and his friendship. The staff members of the Biomedical Engineering at Georgia Tech and Emory have helped me complete this degree. Finally, I am grateful for my friends and family who prayed and encouraged me. I am especially thankful for my wife Yujin for her endless support, patience, and unwaivering love. Thank God for everything.

TABLE OF CONTENTS

LIST OF TABLES

LIST OF FIGURES

SUMMARY

Functional MRI (fMRI) have provided information on networks, disorders, and cognitive performance of the brain. Recent studies have focused on fMRI during resting state (rs-fMRI) without any explicit tasks. To supplement BOLD signals, resting-state fMRI studies have been paired with simultaneous recording of electrophysiology data, a method to provide a direct measure of neural activity. Studies have focused on analyzing infraslow frequencies (< 1Hz) to understand large-scale spontaneous spatial and temporal fluctuations. Dynamic analysis of infraslow frequencies has shown semi-reoccurring BOLD patterns, which have been defined as quasi-periodic patterns (QPP) [1]. This study expands on the previously acquired data [2, 3] using simultaneous fMRI and local field potential (LFP) recordings to understand effects of removing quasi-periodic patterns from the BOLD signal. Furthermore, this study focuses on the impact of quasi-periodic patterns regression on the relationship between BOLD and LFP at multiple frequency bands (infraslow and frequencies between 1 and 100Hz). Results show that the most significant BOLD correlation before QPP regression occurs at the infraslow LFP band. After QPP regression, the stronger BOLD correlation shifts towards the higher LFP frequencies. The reduction in BOLD correlation to LFP after QPP regression suggests that infraslow and higher frequency neural activities contribute to the coordination of large-scale networks observed through quasi-periodic patterns.

CHAPTER 1
INTRODUCTION AND BACKGROUND

Functional MRI (fMRI) studies have been able to provide information on neural networks, neurological disorders, and cognitive performance. Functional MRI indirectly measures neural activity based on the concentration of oxyhemoglobin and deoxyhemoglobin ratio. Magnetic susceptibility of oxygen provides fMRI the necessary signal contrast in the brain. Neurons that are active require more oxygen than those that are inactive. Because the brain doesn't store any energy, increased blood flow and metabolism supply energy to neurons. Through a process called hemodynamic response, the level of oxygenated hemoglobin exceeds the level of deoxygenated hemoglobin within the active neuron. This measured signal from fMRI has been defined as blood oxygenation level-dependent signal (BOLD) [4]. Increased localized blood flow in response to active neurons increases BOLD signal. BOLD signals provide an indirect way to measure local changes in neural activity.

Compared to early studies that focused on task-based fMRI, recent studies have focused on measuring fMRI without any explicit task, which is commonly known as resting-state fMRI. One of the earliest studies demonstrated a difference in BOLD signal between task and resting state fMRI by showing a strong correlation of low frequency (< 0.1Hz) BOLD signals in distinct regions of the human brain [5]. These correlated areas of the brain were named *functional networks* because the regions did not necessarily follow anatomical connections although later studies have shown some functional networks follow anatomical pathways. Some of the most commonly found functional networks in humans were named as *default mode network* and *task-positive networks*. Default mode network includes posterior cingulate cortex, angular gyri, and prefrontal cortex regions during resting conditions whereas task-positive networks (anti-correlated with default mode network) contain re-

gions activated during task-oriented activities [6, 7]. Methods to identify these *functional networks* have been termed *functional connectivity*.

Early studies assumed functional networks to be stationary throughout a fMRI scan. Traditional functional connectivity techniques measured an average estimate of functional networks. However, different experiments have shown that functional networks can vary throughout a scan. Recent studies have focused on dynamic analysis techniques such as sliding window correlation [8, 9] and pattern finding algorithms [1, 10] to conduct dynamic analysis of the brain on a shorter time scale of seconds instead of minutes.

Because of the complexity of BOLD signals, many studies have incorporated other modalities to accompany fMRI scans. One popular method has been simultaneous fMRI-EEG studies to noninvasively measure electrical activity in human and primate [11, 12, 13]. Multi-modal studies have provided a way to verify and understand neural origins of BOLD signals. Studies in rodents [13, 2, 14, 15], monkeys [11], and humans [10, 16] have shown highly structured spatial correlations in distinct areas of the brain. Functional connectivity has shown differences between healthy and patients with brain disorders such as Alzheimer, schizophrenia, depression, and autism [8, 17, 16]. Relationships have also been established between functional networks and behavior through studies of language and memory. Evidence have demonstrated neural activity drives functional connectivity.

Simultaneous fMRI and intracortical neurophysiological recordings have provided more localized measurements of BOLD and neural activity. Our lab has focused on developing concurrent fMRI and intracortical electrophysiology experiments to provide more localized electrical measurements compared to EEG studies. Simultaneous fMRI and local field potential (LFP) recordings have shown infraslow frequencies have strong correlation to BOLD signals and greater interhemispheric correlation [13]. Invasive microelectrode

animal recordings have shown that gamma-band activity is linked to local BOLD signals [11]. These studies with invasive microelectrodes have demonstrated spontaneous BOLD fluctuations to correlate with electrical activity. Studies with fMRI and neurophysiological recordings have provided additional insight into the relationship of BOLD signals to neural activity.

Recently, more studies have shifted towards investigating infraslow frequencies ($<$ 1Hz) [13, 14, 15] to understand large-scale spatial and temporal organizations of the brain. Past limitations in amplifier hardware have prevented studies on infraslow frequencies. However, recent developments in simultaneous fMRI and neurophysiological recordings have shown infraslow frequencies have strong correlation to BOLD signals [13, 2]. One possible source of the strong correlation between infraslow BOLD and LFP signals has been linked to semi-reoccurring patterns called Quasi-periodic patterns (QPPs) [10, 2]. QPPs have been revealed in resting-state fMRI signals for rats and humans. For rats, QPPs tend to propagate from ventral-lateral to dorsal medial cortex [1, 2]. For humans, QPPs alternate between default mode and task- positive networks, which are associated with attention and cognitive processing [10]. Studies have suggested infraslow LFP signals play an essential role in the coordination of large-scale BOLD fluctuations shown through QPPs.

BOLD signals reflect multiple electrical activities of the brain whereas QPP signal has been shown to be driven primarily by infraslow neural activity. The motivation of this study explores the BOLD signal after removal of the QPP signal. Does the remaining signal become more closely linked to higher frequency neural activity? Furthermore, this study addresses whether higher frequencies drive QPP in addition to infraslow electrical activity. This study expands on previously acquired data in our lab [13, 2] by removing QPP components from the BOLD signal with a linear regression method and analyzing the effects on correlation to electrophysiology data. Changes to infraslow BOLD signals with

and without QPP regression were correlated with different LFP bands including infraslow, delta, theta, alpha, beta, and gamma under isoflurane and dexmedetomidine anesthesia. By comparing changes before and after QPP regression, the study expected QPP regression to remove QPP component from the BOLD signal and significantly reduce correlation to electrophysiology data although the degree of reduction may differ for different LFP bands.

The results showed that infraslow frequency band has the strongest correlation to BOLD before QPP regression. After QPP regression, the BOLD signal becomes more closely linked to the higher frequencies although the results are unclear due to the small correlation values. Furthermore, the study showed that both infraslow and higher frequency neural activity play a role in coordinating large-scale networks observed in the QPPs.

CHAPTER 2

TECHNICAL APPROACH

2.1 Data Preparation and Recording

2.1.1 Animal Preparation and Anesthesia

Ten rats underwent simultaneous fMRI-LFP scans with either isoflurane or dexmedetomidine anesthesia. These two anesthesia have been widely used in rats for functional connectivity research [18, 3]. Animal preparation and recordings were approved by Emory University Institutional Animal Care and Use Committee. Six rats were recorded between 1.3% to 2.0% isoflurane. Four of those rats underwent additional scans with dexmedetomidine anesthesia after isoflurane scans. Remaining rats were recorded with dexmedetomidine. An initial 0.05mg/kg bolus of dexmedetomidine was injected and then continued with 0.1mg/kg/hour infusion [12, 3]. Between 2 and 15 simultaneous fMRI-LFP scans were recorded for each rat. Physiological parameters were aligned with the protocol for isoflurane and dexmedetomidine anesthesia. Body temperature averaged at $37.0\,^{\circ}\mathrm{C}$ under isoflurane and $37.1\,^{\circ}\mathrm{C}$ under dexmedetomidine. Breathing rate averaged at 56.9 breaths per minute with isoflurane and 84.3 breaths per minute with dexmedetomidine.

2.1.2 fMRI Data Recording

With anesthetized rats, fMRI BOLD data was recorded on a 9.4T Bruker animal scanner using a volumetric transition coil and 2cm surface receiver coil. BOLD data was acquired with ParaVision 4.0, gradient echo planar imaging (EPI), TR 500ms (2Hz), TE of 15ms, 2mm slice, FOV of 1.92x1.92cm, and a matrix size of 64x64. 500 seconds of BOLD signal were recorded for each scan.

2.1.3 Local Field Potential (LFP) Data Recording

For LFP recordings, silver/silver chloride glass microelectrodes were inserted to the left and right primary somatosensory cortex of forelimb region (S1FL). Direct-current amplifiers were used to record low-frequency content from electrodes. Microelectrodes acquired data at a sampling frequency of 12kHz from left and right S1FL regions. LFP recording began a few seconds before fMRI acquisition and ended a few seconds afterward.

2.2 Data Processing Flowchart

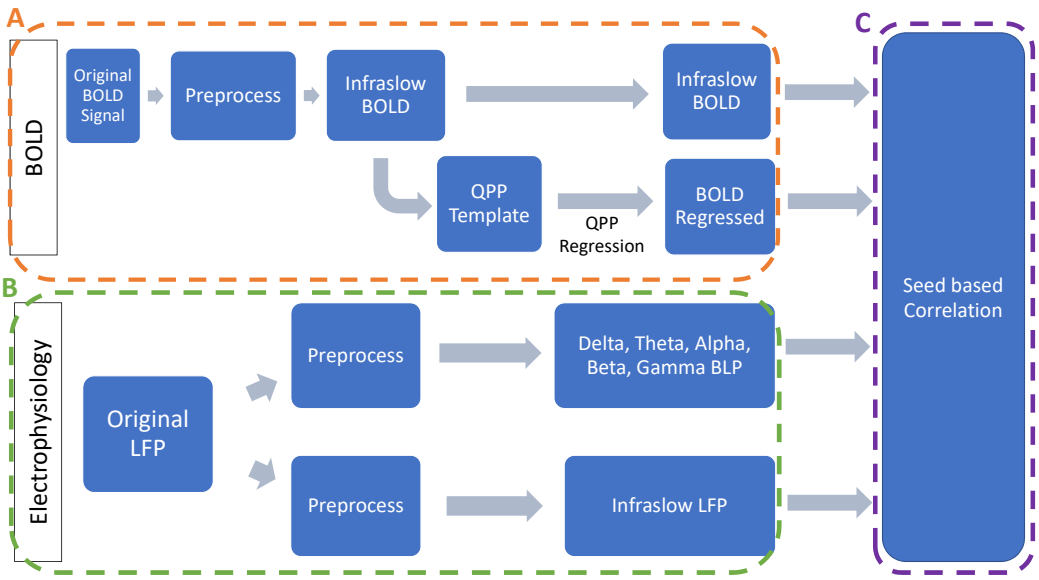

Figure 2.1: Flowchart. Part A illustrates the steps to process the BOLD signal into infraslow and BOLD regressed signal. Part B shows the steps to separate the LFP data into different frequency bands. Part C demonstrates the relationship between BOLD and electrophysiology through seed-based correlation.

2.3 Part A: Process BOLD Signal

2.3.1 A1: Extract Infraslow BOLD

To obtain infraslow BOLD signal, the following steps were applied to the original fMRI BOLD signal (Fig. 2.2). For each voxel within the rat brain, fMRI BOLD signal was re-

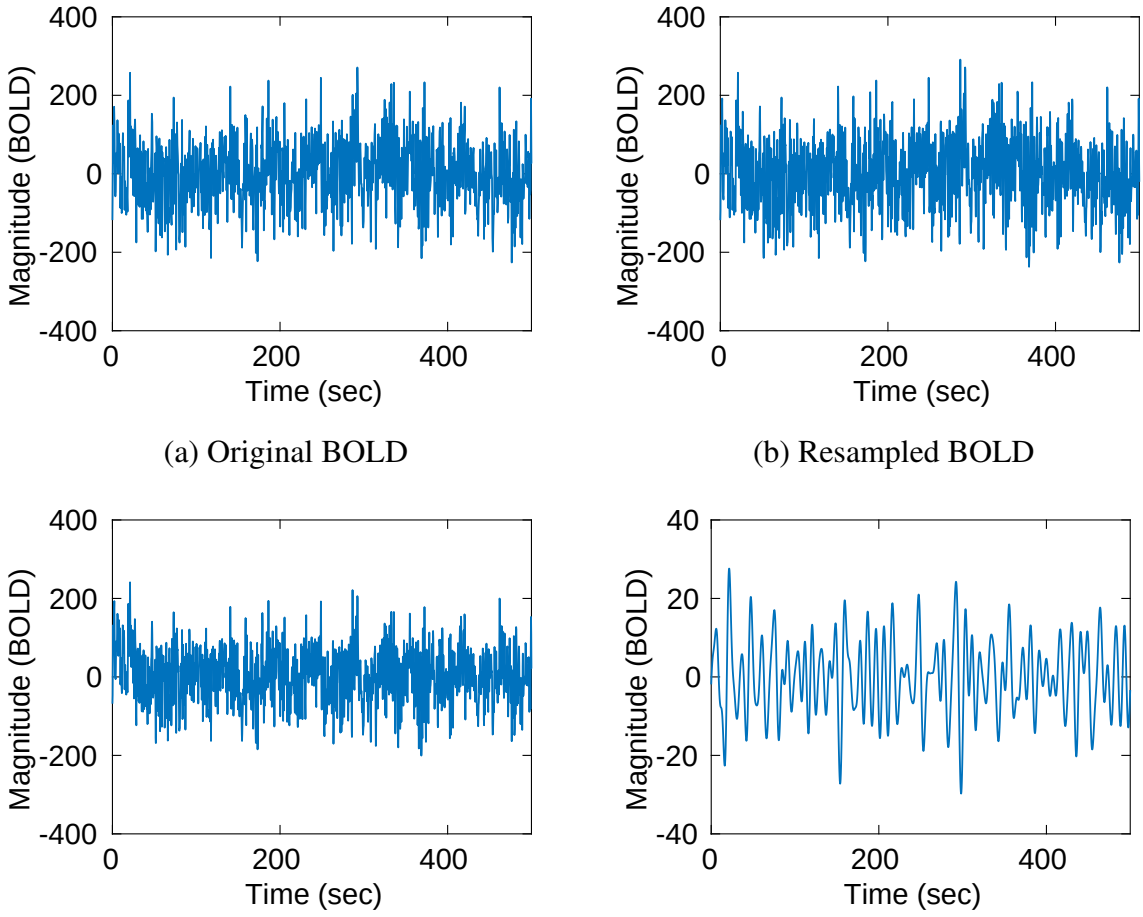

(a) Original BOLD

(b) Resampled BOLD

(c) Detrended BOLD

(d) Filtered and Normalized BOLD

Figure 2.2: Preprocessed BOLD Infraslow for Rat1 Scan2 with isoflurane anesthesia. Figures a-d display BOLD signal over the entire 500 second scan for left ROI region of the rat brain (primary somatosensory cortex S1FL). (a) Original BOLD signal over the entire 500 second scan time that was acquired with gradient echo planar imaging (EPI), TR 500ms (2Hz), and TE of 15ms. (b) Resampled BOLD signal from 2Hz to 4Hz. (c) Detrended with zero-phase 4th order high-pass IIR filter with a passband frequency of 0.01Hz. (d) Filtered BOLD signal to infraslow frequencies using empirically derived filter and normalized to mean zero.

sampled to 4Hz. Detrending was performed by zero-phase fourth order high-pass infinite impulse response (IIR) filter with a passband frequency of 0.01Hz. The last data point of the resampled BOLD signal was cropped to match the size of LFP data. Based on a previous study, an empirical filter performed better than a standard box filter for infraslow frequencies [2]. This empirical filter was calculated based on magnitude squared coherence between each electrode's LFP and BOLD signal using the same dataset. Peaks from mean coherence spectra were used to develop the empirical filter for each anesthesia. The empirical filter in this study has a pass-band of 0.038-0.184Hz for isoflurane and 0.045-0.304Hz for dexmedetomidine. Further details are shown in the study by Thompson et al [2]. The filtered BOLD signal was normalized to mean zero as the final step to preprocessed BOLD signal.

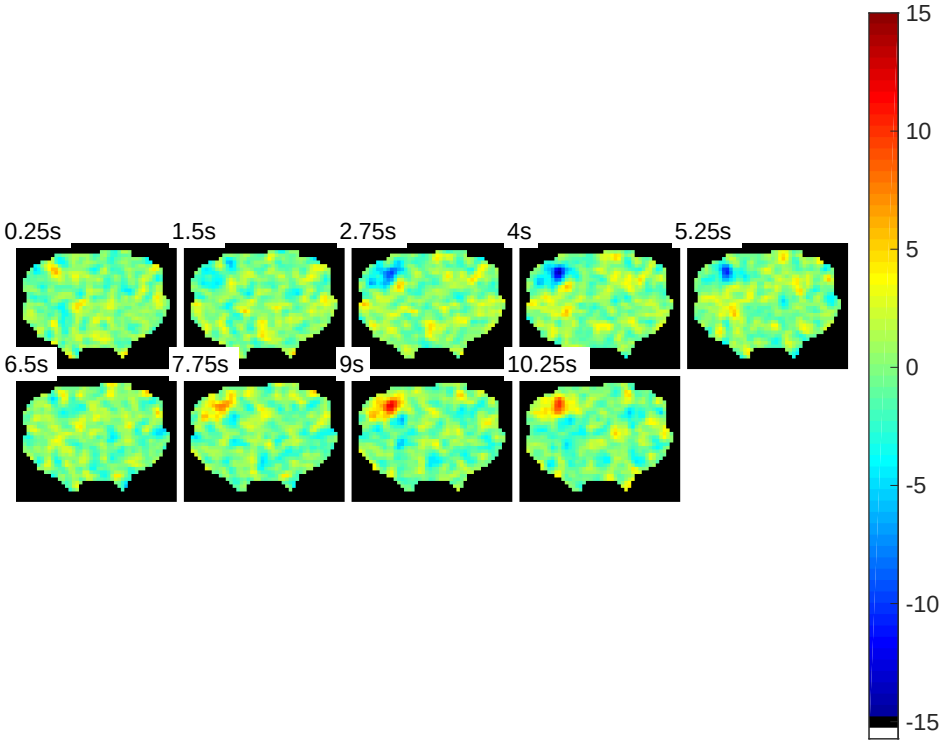

Figure 2.3: QPP Template images Rat1 Scan2 in isoflurane conditions. Images display the final QPP template extracted from Rat1 Scan2. Images display QPP template at different time points: 1.25 second interval time points ranging from 0.25 to 10.25 seconds. The BOLD signal fluctuates more in the left S1FL region and not in the right region. The scale ranges from -15 to 15.

2.3.2 A2: Extract Quasi-periodic pattern template from Infraslow BOLD

The BOLD signal was exclusively used to extract quasi-periodic pattern (QPP) templates (Fig. 2.3). This algorithm was developed in our lab as shown in the paper by Majeed et al [1]. This algorithm first selected an initial template based on a starting point and calculated correlation of the initial template over the entire duration of the scan. Sections of the BOLD signal with correlations above the thresholds were averaged together and updated to be the template for the next iteration. These steps were repeated multiple times with the updated templates. Correlation thresholds peaks were set to a low value of 0.001 for the first three iterations and 0.002 for the remaining iterations up to a maximum of 10,000 iterations to ensure convergence. The final template was determined when the previous and updated correlation time series does not change. As mentioned before, the QPP extraction step was only based on preprocessed BOLD data and does not include any information from LFP data.

Parameters chosen for this algorithm were unique and may be different for other studies. The initial QPP template was selected at approximately 62.5 seconds into the BOLD signal. Different starting points were shown not to influence the final QPP template results [2]. The inverse of the empirical filter frequency center of mass was used to determine the template length parameter. With a 0.088Hz frequency center of mass from the isoflurane empirical filter, template length was set to 11.25 seconds. With a 0.15Hz frequency center of mass from the dexmedetomidine empirical filter, the template length was set to 6.50 seconds. Furthermore, the region of interest (ROI) for the QPP template algorithm was set to both left and right S1FL regions, which were manually drawn using a rat brain atlas as a comparison. QPPs were less prevalent in the right S1FL region and excluded from further analysis. The lack of QPPs in the right S1FL may have been due to inaccurate LFP recordings of the right electrode.

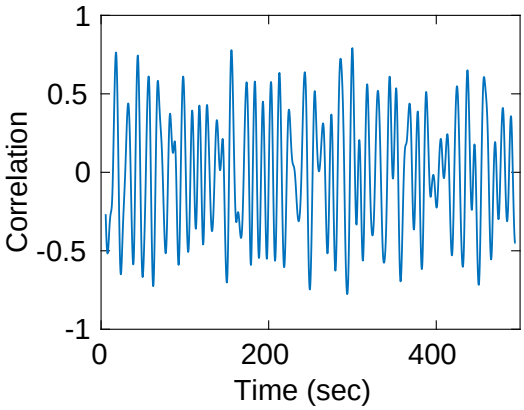

(a) Correlation Strength

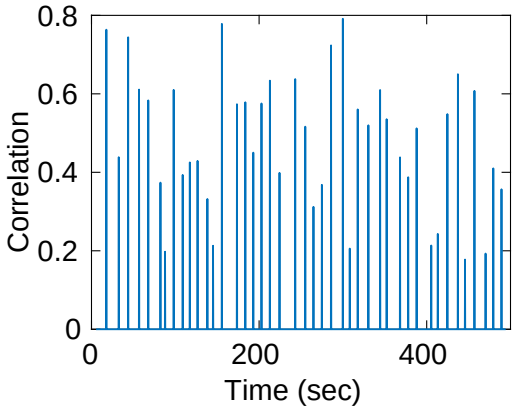

(b) Correlation seed time points

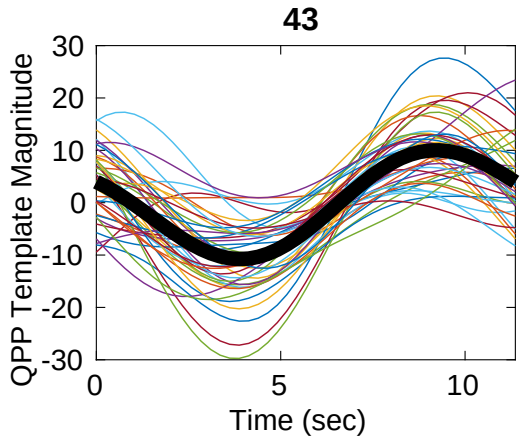

(c) QPP Templates - left S1FL

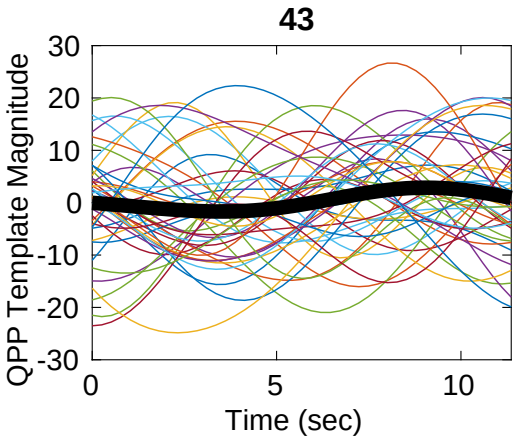

(d) QPP Templates - right S1FL

Figure 2.4: Quasi-periodic pattern (QPP) correlation and ROI time series. (a) Correlation QPP strength. (b) Peak correlation seed timepoints that are above the QPP template threshold used on the final iteration to calculate the final QPP template. (c) Left ROI of the QPP template. Colored lines illustrate the left ROI QPP template time series that was used to calculate the final QPP template (Black line). (d) Right ROI QPP template time series to estimate the final QPP template.

2.3.3 A3: Remove QPP components from Infraslow BOLD using Linear Regression

$$Y = X\beta, \tag{2.1}$$

$$Solve : \min_{\beta} ||Y - X\beta||^2, \tag{2.2}$$

$$Solution : \hat{\beta} = (X^T X)^{-1} X^T Y \tag{2.3}$$

$$\hat{Y} = X\hat{\beta} \tag{2.4}$$

$$Regression : Z = Y - \hat{Y} \tag{2.5}$$

where each variable represents one pixel:

Y = BOLD Signal Time Vector

X = Regressor (Normalized QPP) Time Vector

β = Regression Coefficient (Scaling Factor) Value

$\hat{Y}$ = Scaled Regressor (Estimated QPP Component) Time Vector

Z = BOLD QPP Regressed Time Vector

QPP regression was an important step to understand changes that occur when removing QPP content from BOLD signal (Fig. 2.5). This step involved a linear regression technique by assuming a general linear model of the BOLD signal as a time vector at one pixel (Eq. 2.1). The Regressor vector (X) was calculated by convolving QPP template by the QPP correlation strength and normalizing by z score at the same pixel. The generalized least-squares minimization problem solved for a (β) regression coefficient that minimizes the error between the scaled regressor ($\hat{Y}$) and preprocessed BOLD signal (Y) (Eq. 2.3). Regressor vector (X) was multiplied by the regression coefficient (β) to calculate the scaled regressor ($\hat{Y}$), which is an estimate of the QPP component from the BOLD signal (Eq. 2.4). To remove the QPP component, the scaled regressor ($\hat{Y}$) was subtracted from BOLD

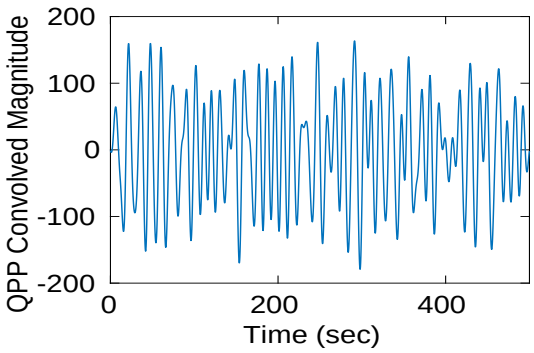

(a) QPP Convolved left ROI

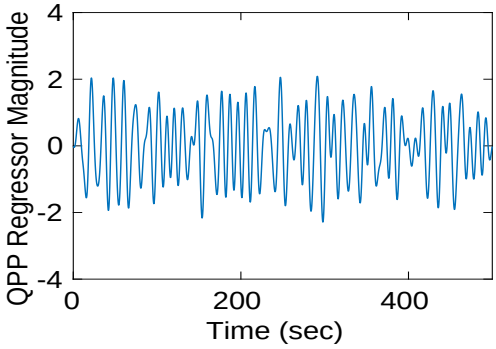

(b) Regressor (X) left ROI

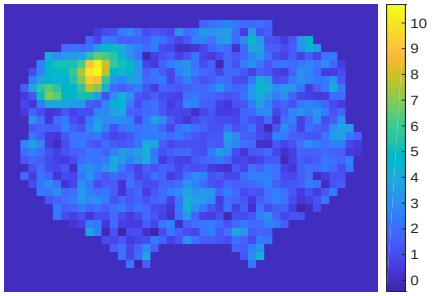

(c) Regression coefficient (β_i)

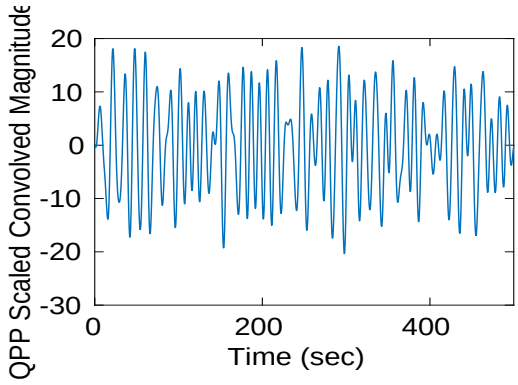

(d) Scaled convolved QPP template ($\hat{Y}$) left ROI

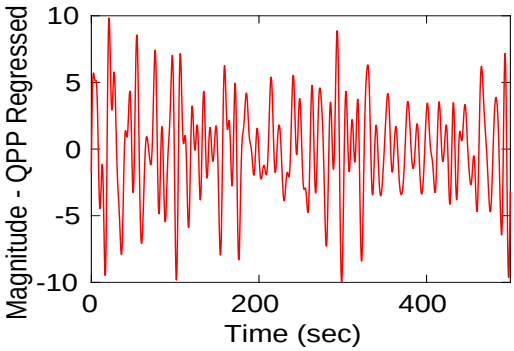

(e) QPP regressed (Z) left ROI

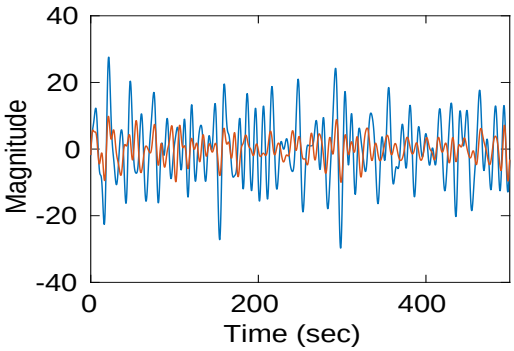

(f) BOLD before & after QPP regression

Figure 2.5: QPP regression of left S1FL region. (a) QPP template convolved with QPP correlation strength showing left ROI. (b) Regressor (X) calculated by taking z score of the QPP convolved time series. (c) Regression coefficients (β_i) for each pixel of the entire rat brain. (d) Scaled Convolved QPP template ($\hat{Y}$) estimated by multiplying the regressor by the regression coefficient. (e) BOLD signal after QPP regression (Z). (f) Comparison of the BOLD signal of left ROI before and after QPP Regression. The blue signal indicates the BOLD signal before QPP regression (Y). The red signal indicates BOLD signal after QPP regression (Z).

signal (Y) (Eq. 2.5). The same steps were repeated for each pixel within the entire brain to remove the QPP component from the BOLD signal.

The regression coefficient β spatial map showed higher β values at the left S1FL region compared to the small β values at the right S1FL region (Fig. 2.5c). The high β value illustrates the Y and X vectors at pixel have similar patterns but differ in a scaling factor. In other words, the QPP component is higher at the pixels with higher β coefficients. On the other hand, low β value indicates the Y and X vectors have very different patterns, and the QPP component is very small.

2.4 Part B: Process Electrophysiology LFP Data

2.4.1 B1: Extract Infraslow LFP

LFP data artifacts were removed by averaging the period between each repetition time (TR). This noise template was created and subtracted for each scan. Further information on artifact removal technique can be found in the paper by Pan et al [13]. Only data recorded with high dose isoflurane between 1.7% to 2.0% were selected for further analysis. High dose isoflurane has been shown in previous studies to have spontaneous BOLD fluctuations [19]. For dexmedetomidine, data recorded at least two hours after switching from isoflurane were considered in the analysis. One previous study showed two hour is necessary to have a stable state to measure spontaneous BOLD activity under dexmedetomidine [20].

To extract infraslow frequency, LFP data was resampled to 4Hz (0.25sec period) with an anti-aliasing filter to match the sampling frequency of the BOLD signal. The same detrending method using highpass IIR filter with 0.01Hz passband frequency was applied to the resampled LFP data to reduce effects of signal drift. Then, LFP data was filtered to infraslow frequencies using the empirical filter as mentioned before. Filtered data then went through a normalization to set mean signal to zero. Final infraslow LFP data matched

the same number of BOLD data points.

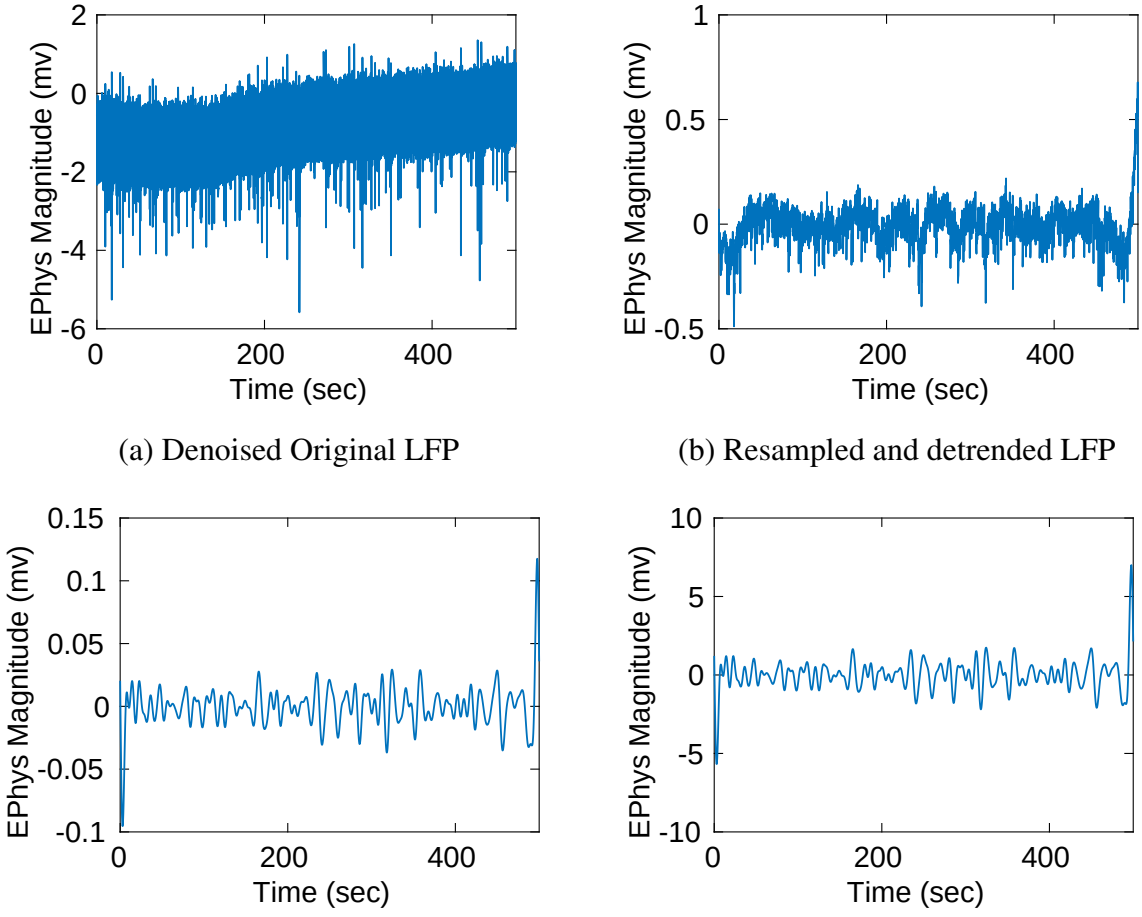

(a) Denoised Original LFP

(b) Resampled and detrended LFP

(c) Filtered infraslow LFP

(d) Normalized infraslow LFP

Figure 2.6: Preprocessed LFP infraslow Rat1Scan2 isoflurane. Figures a-d display LFP signal of the left electrode. (a) Denoised LFP signal sampled at 12kHz and acquired at the left electrode (left S1FL region) (b) 4Hz resampled LFP signal to match the sampling frequency of the pre-processed BOLD signal. Detrended with zero-phase 4th order high-pass IIR filter with a passband frequency of 0.01Hz. (c) LFP filtered to infraslow frequencies using the same empirically derived filter. (d) Normalized Infraslow LFP signal to mean zero.

2.4.2 B2: Extract BLP High Frequency LFP

To push the boundaries of the original scope of the study, bandlimited power (BLP) was analyzed to study the relationship of QPP regression with higher LFP frequencies. Original LFP data underwent the same noise and artifact removal technique as before. Detrending

was applied with a zero-phase fourth order highpass IIR filter with 0.8Hz passband frequency. Then, LFP signal was bandlimited to frequencies of interest: delta (1-4Hz), theta (4-8Hz), alpha (8-16Hz), beta (16-32Hz), and gamma (32-100Hz). These bands have been commonly analyzed with electrophysiology data. LFP signals were filtered in the Fourier domain to band-limit the LFP to different higher frequencies.

For the higher LFP frequencies, LFP data was divided into two second window. A two second window was necessary to span at least one cycle for all higher frequencies. Furthermore, each BLP calculation corresponded to the same time point of the infraslow BOLD signal. Hence, BLP estimation matched the 4Hz BOLD sampling rate. For each two second window, mean power spectral density was calculated using power spectrograms. BLP calculation provided a way to capture the envelope of power fluctuations. The same empirical filter was applied to BLP signal and normalized to mean zero. Filtering higher BLP frequencies to the infraslow frequencies using the same empirical filter was a necessary step in this study. Because of significant differences in oscillation timescale between BOLD and higher LFP frequencies, the empirical filter was applied to BLP to have a better comparison to the infraslow BOLD signal.

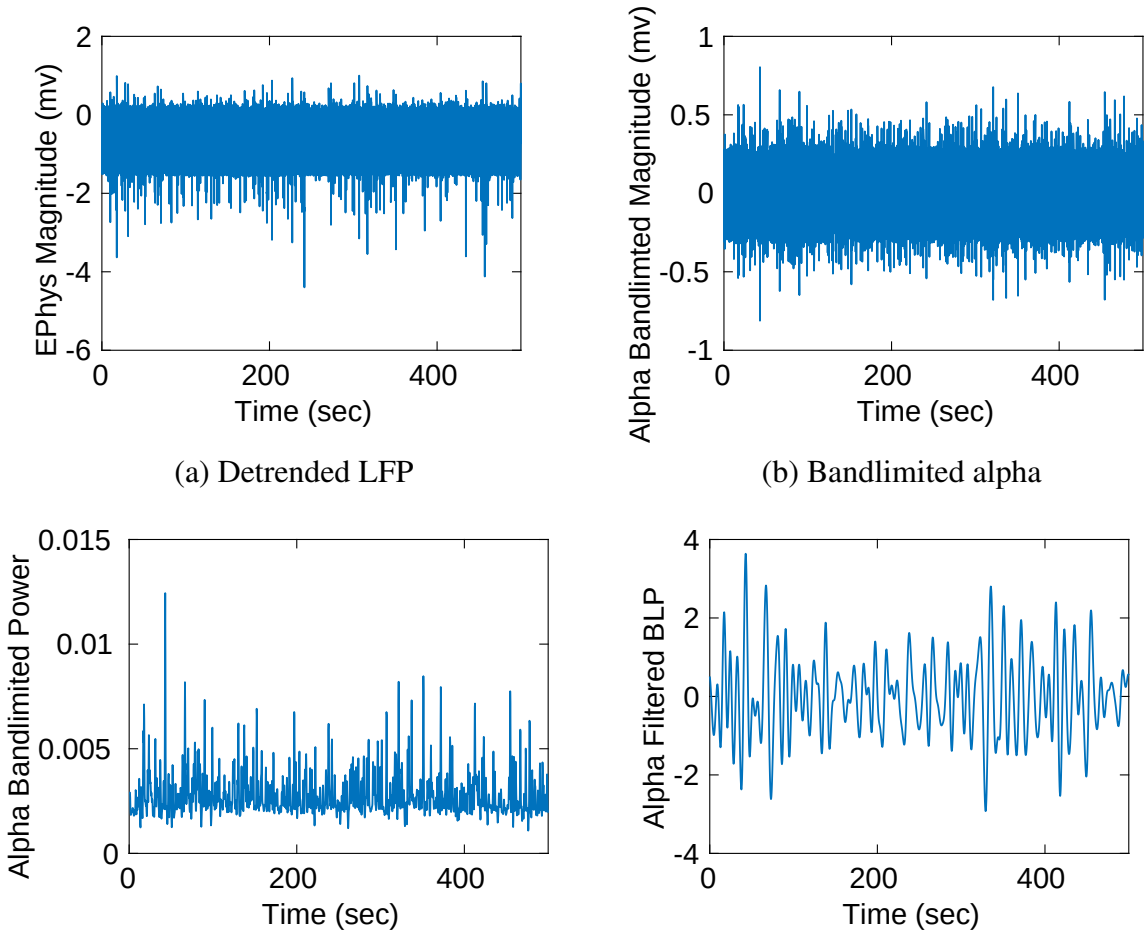

(a) Detrended LFP

(b) Bandlimited alpha

(c) Bandlimited alpha power

(d) Empirical filtered Alpha BLP

Figure 2.7: Preprocessed alpha LFP Rat1 Scan2 in isoflurane conditions. Figures a-d display preprocessing steps for left alpha LFP data. (a) Detrending with a zero-phase fourth order highpass IIR filter with 0.8Hz passband frequency. (b) Bandlimiting alpha signal frequencies (8-16Hz) using Fourier transformation and recovering alpha time signal. (c) Alpha bandlimited power (BLP) by calculating the mean power of the power spectrogram for each two second window. (d) Filtering alpha BLP with the empirically derived filter.

2.5 Part C: Correlation Analysis

Frequency	BOLD Correlation	BOLD Regressed Correlation
Infraslow	r-BOLD-Infraslow	r-Infraslow-BOLDRegress
Delta	r-BOLD-Delta	r-BOLDRegress-Delta
Theta	r-BOLD-Theta	r-BOLDRegress-Theta
Alpha	r-BOLD-Alpha	r-BOLDRegress-Alpha
Beta	r-BOLD-Beta	r-BOLDRegress-Beta
Gamma	r-BOLD-Gamma	r-BOLDRegress-Gamma

Table 2.1: List of time-lagged correlation for each BOLD-LFP pair. Six different LFP signal correlated with BOLD. Same LFP signals correlated with BOLD after QPP regression. Total of 12 different time-lagged correlations.

A seed-based functional connectivity analysis was performed at different time lags to provided a method to determine any spatial and temporal relationships between BOLD and LFP signal. Seed signal was set as the left LFP and correlation was calculated over the entire rat brain at different time lags. Pearson correlation coefficient (PCC) was used to analyze the relationship between BOLD and BLP at various time lags. For each voxel within the rat brain, Pearson correlation was calculated between BOLD and LFP electrode with time shifts between -10 to 10 seconds. The range of time shift was sufficient to capture localized correlations. A similar analysis was demonstrated in a previous study by Thompson et al [2]. Due to abnormal correlations at the edges of the signal, 10 seconds at the beginning and end were excluded in time-lag correlations. The time-lag correlation was calculated for r-BOLD-Infraslow and r-BOLDRegress-Infraslow to compare effects of regression on correlation for infraslow frequencies. The same time-lag correlation was calculated for higher BLP frequencies. As stated in the previous study on the same dataset, the sign of correlation coefficient between infraslow LFP and infraslow BOLD was reversed because the bursting direction was recorded downwards [21, 2]. Sign reversal was not applied to correlation between BOLD and higher BLP frequencies because BLP is not influenced by the direction of the power fluctuations. The final list of the different time-

lagged correlation is shown in Table 2.1.

2.6 Significance Testing

Significance was determined using a paired one-sided t-test. Peak correlation before and after QPP regression was compared to determine a statistical difference. The null hypothesis tests whether the true mean difference is less or equal to zero. Only the left ROI was included in the analysis. The comparison was tested with a significance level of 0.01.

CHAPTER 3

RESULTS

Data was acquired from ten Sprague-Dawley rats. Four rats underwent isoflurane conditions and seven rats underwent dexmedetomidine conditions. Two glass electrodes were inserted in left and right primary somatosensory cortex (S1FL) region. After discarding scans that did not fall within appropriate isoflurane and dexmedetomidine criteria, 14 total scans were analyzed for isoflurane and 46 total scans for dexmedetomidine anesthesia.

Furthermore, third-party matlab code was used to plot figures. "PlotPub.m" function by K M Masum Habib was used to plot figures (`https://github.com/masumhabib/PlotPub`) and "boundedline.m" function by Kelly Kearney was used to plot shaded error bars (`https://github.com/kakearney/boundedline-pkg`).

3.1 Quasi-periodic Patterns

Individual QPP templates were generated for all rats and scans using the algorithm developed by Majeed et al [1]. The pattern finding algorithm extracted a semi-reoccurring spatial and temporal pattern within the left and right S1FL region. In some cases, the QPP algorithm found a distinct quasi-periodic pattern in both left and right S1FL regions. Often, the algorithm extracted a distinct pattern in only one region, mainly in the left S1FL region. In this case, QPP existed primarily in the left S1FL region, which was used for further analysis. As mentioned before, QPP templates were generated only from BOLD signals without any information from electrophysiology data.

3.2 LFP Bandlimited Power (BLP)

To analyze the relationship of BOLD before and after QPP regression to higher LFP frequencies, LFP was bandpass filtered to frequencies of interest. Then, average bandlimited power (BLP) was estimated within each window over the entire scan time. Setting a 0.25 seconds window length to calculate gamma bandlimited power resulted in BLP signal to be at the noise level. Thus, two second windows were chosen to capture enough oscillation of LFP signal to accurately estimate power even though power estimation includes overlapping regions as shown in a small offset in the BLP estimation (Fig. 2.7). A larger window of two seconds provided a BLP estimation that reduced effects of noise.

3.3 Time-lagged BOLD-LFP Spatial Correlation maps - Isoflurane

Spatial BOLD time-lagged correlation of Rat1 Scan2 was analyzed for BOLD before (r-BOLD-Infraslow) and after QPP regression (r-BOLDRegress-Infraslow) under isoflurane conditions (Fig. 3.1 and 3.2). For seed-based functional connectivity calculation, seed signal was set as the left electrode infraslow LFP for these specific figures. Time-lag correlation for BOLD before QPP regression showed dynamic changes of BOLD signal throughout time (Fig. 3.1) with the greatest change especially prominent in the S1FL left region. In this particular example, BOLD coherence was not observed between left and right S1FL regions although some scans showed coherence between interhemispheric regions. Time-lag correlation varied from negative to positive with a positive peak correlation occurring at 3.75 seconds. These BOLD spatial correlation maps were drastically different after QPP regression (Fig. 3.2). Correlation values within the left S1FL regions were significantly smaller and not prominent in the BOLD-Regressed spatial correlation maps. With QPP regression, correlation coefficients between infraslow LFP frequency and infraslow BOLD-Regressed signal were significantly reduced.

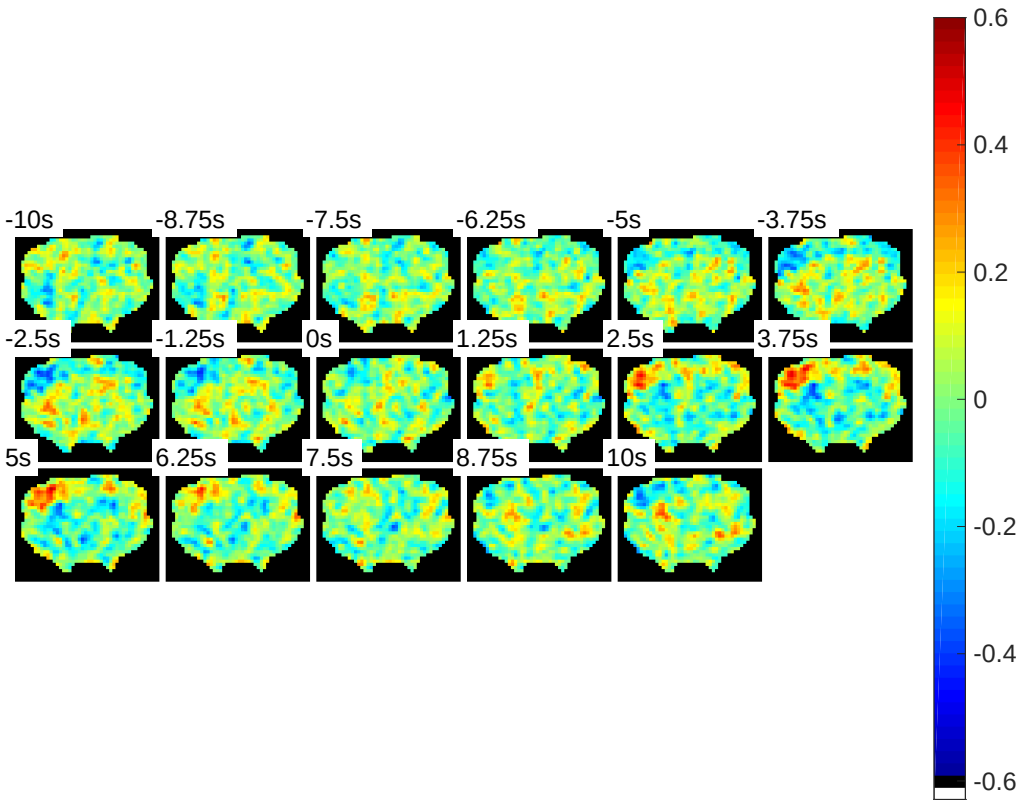

Figure 3.1: Infraslow BOLD images time-lag correlation before QPP regression - isoflurane Rat1 Scan2. This figure illustrates changing correlation that occurs between preprocessed infraslow BOLD signal and infraslow LFP signals over the entire rat brain as a function of time lag. A seed-based correlation was performed on the whole brain, and seed signal was set as the left LFP infraslow signal. In this particular rat and scan, correlation values within the left S1F1 region had a positive peak correlation at 3.75 seconds time-lag. Images display time-lag correlation values between -10 and 10 seconds with intervals of 1.75 seconds. The correlation scale ranges between 0.6 and -0.6.

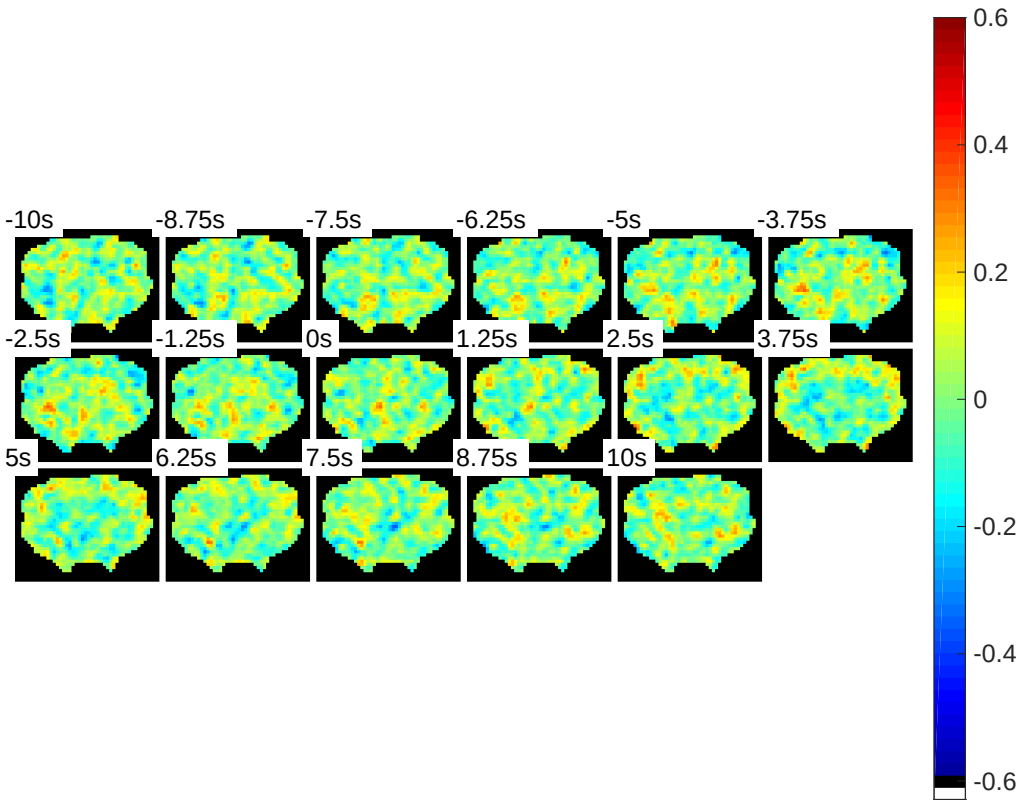

Figure 3.2: Infraslow BOLD images time-lag correlation after QPP regression - isoflurane Rat1 Scan2. This figure is a direct comparison to Figure 3.1 to illustrate changes in BOLD time-lag correlation after QPP regression. A seed-based correlation was performed on the whole rat brain, and seed signal was set as the left LFP infraslow signal. With QPP regression, correlation values were significantly reduced over the whole rat brain region. Images display time-lagged correlation values between -10 and 10 seconds with intervals of 1.75 seconds.The correlation scale ranges between 0.6 and -0.6.

3.4 Time-lagged BOLD-LFP Spatial Correlation maps - Dexmedetomidine

Spatial maps of time-lag correlation were also analyzed for dexmedetomidine conditions (Fig. 3.3 and 3.4). These figures showed time-lag correlation of the entire rat brain before (r-BOLD-Infraslow) and after QPP regression (r-BOLDRegress-Infraslow) under dexmedetomidine conditions. As before, seed-signal was set as the left infraslow LFP signal, and seed-based functional connectivity analysis was performed over the entire rat brain. Correlation varied from positive to negative within the positive time-lags. For this

particular scan, peak correlation for r-BOLD-Infraslow was located at 1.25 second time lag. Compared to isoflurane anesthesia, different areas of the brain showed coherence to the left S1FL (Fig. 3.3). QPP regression decreased the overall correlation of r-BOLDRegress-Infraslow throughout the entire cortex.

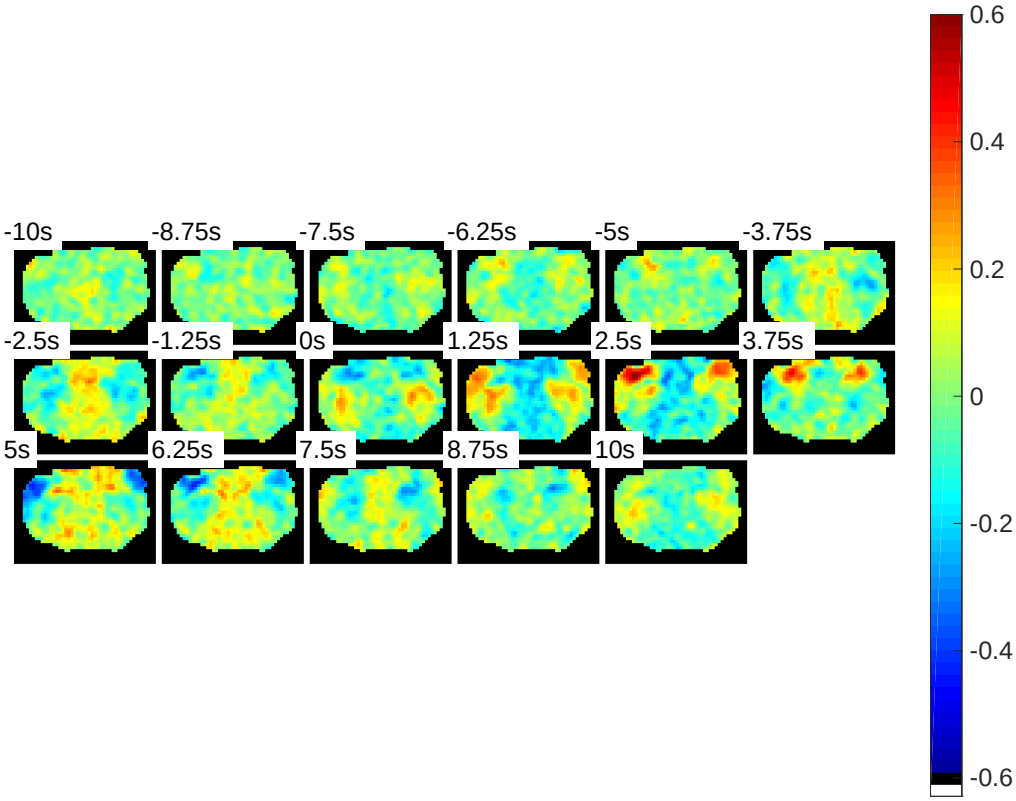

Figure 3.3: Infraslow BOLD images time-lag correlation before QPP regression - dexmedetomidine for Rat4 Scan2. A seed-based correlation was performed over the entire rat brain, and seed signal was set as the left LFP signal. This figure illustrates changing correlation that occurs between preprocessed infraslow BOLD signal and infraslow LFP signals over the entire rat brain as a function of time lag under dexmedetomidine anesthesia. In this particular rat and scan, correlation values within left S1F1 region had peak correlation at 2.5 seconds time-lag. Images display time-lag correlation values of the entire rat cortex between -10 and 10 seconds with intervals of 1.75 seconds. The correlation scale ranges between 0.6 and -0.6.

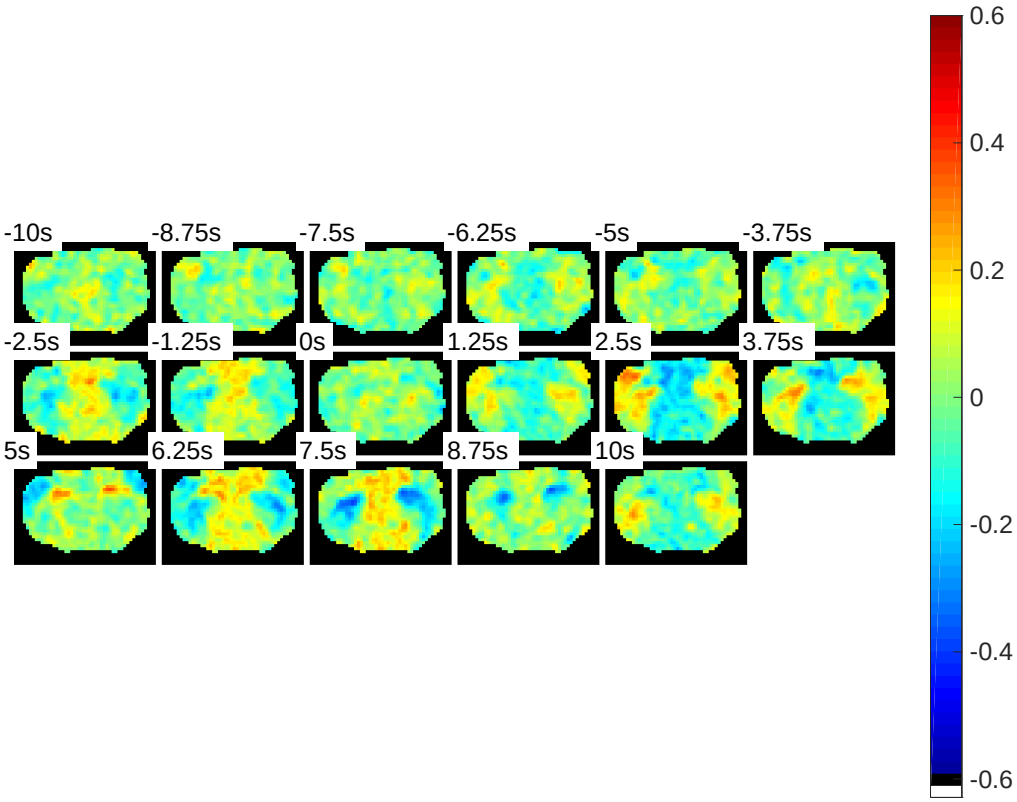

Figure 3.4: Infraslow BOLD images time-lag correlation after QPP regression - dexmedetomidine for Rat4 Scan2. A seed-based correlation was performed over the entire rat brain, and seed signal was set as the left LFP electrode. This figure is a direct comparison to Figure 3.3 to illustrate changes in time-lag correlation after QPP regression. With QPP regression, correlation values were significantly reduced over the entire rat brain region. Images display time-lagged correlation values of the entire rat cortex between -10 and 10 seconds with intervals of 1.75 seconds. The correlation scale ranges between 0.6 and -0.6.

3.5 Time-lagged BOLD-LFP for All Scans - Isoflurane

To understand the relationship between BOLD and LFP signal, time-lag BOLD-LFP correlation was analyzed for all scans and multiple LFP bands under isoflurane (Fig. 3.5). These plots were generated by calculating the left S1FL time-lag correlation using the left electrode as the seed signal. For isoflurane conditions, peak BOLD correlations for all different LFP were found within the positive time-lag which align with a previous study [13]. Left S1FL region overall exhibited strong BOLD correlation (Tab. 3.1) for all LFP frequency bands. Maximum BOLD-LFP correlations for all LFP frequency bands ranged between 3.25 and 5 second time-lag. After QPP regression, greatest correlation change occurred between r-BOLD-Infraslow and r-BOLDRegress-Infraslow in the left S1FL region. Mean maximum correlation decreased by 0.13 (Fig. 3.1). Overall, the trend showed QPP regression decreases correlation for all LFP frequency bands under isoflurane anesthesia.

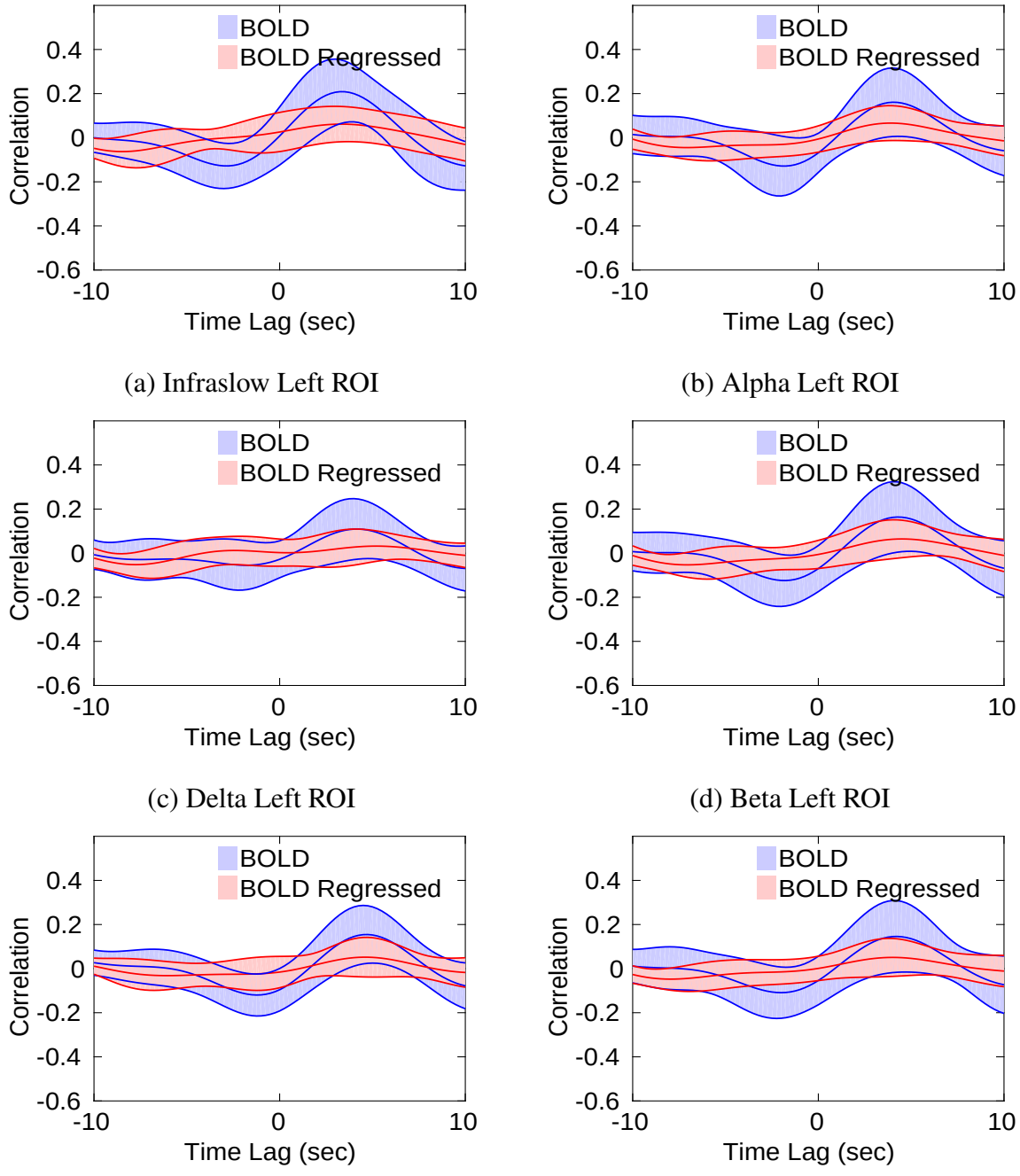

(a) Infraslow Left ROI

(b) Alpha Left ROI

(c) Delta Left ROI

(d) Beta Left ROI

(e) Theta Left ROI

(f) Gamma Left ROI

Figure 3.5: Time-lag correlation left ROI - isoflurane. Time-lag cross correlation of the left S1FL regions before (Blue) and after (Red) QPP Regression for all rats and scans in isoflurane conditions. Positive time-lag indicates LFP preceded BOLD signal. The plot illustrates mean (middle curve) and one standard deviation (outer curve) of correlation for all scans using isoflurane. The correlation scale ranges between 0.6 and -0.6. Time-lag ranges between -10 and 10 seconds.

Table 3.1: Time-lag maximum correlation results of the left S1FL - isoflurane.

	BOLD Before QPP		BOLD After QPP		BOLD Corr Diff	
LFP	Time-lag (sec)	Peak Correlation	Time-lag (sec)	Peak Correlation	Time-lag (sec)	Peak Correlation
Infraslow	3.3	0.21 ± 0.15	3.3	0.06 ± 0.08	3.3	0.15 ± 0.11
Delta	4.3	0.11 ± 0.14	5.3	0.03 ± 0.07	3.8	0.08 ± 0.09
Theta	4.8	0.16 ± 0.13	4.5	0.05 ± 0.09	4.8	0.10 ± 0.10
Alpha	4.0	0.16 ± 0.16	4.0	0.07 ± 0.08	4.3	0.10 ± 0.12
Beta	4.3	0.16 ± 0.16	4.5	0.06 ± 0.09	4.3	0.10 ± 0.13
Gamma	4.3	0.15 ± 0.16	4.0	0.05 ± 0.08	4.3	0.10 ± 0.13

This table is based on results shown in Figure 3.5. Maximum mean time-lag correlation (Max r-BOLD-LFP) was calculated, and time-lag location (Time-Lag (Sec)) of the maximum correlation was determined for each LFP band within the left S1FL region. Maximum time-lag correlation and the corresponding time-lag location for BOLD regressed (r-BOLDRegress-LFP) was calculated. Lastly, the maximum difference in correlation between r-BOLD-LFP and r-BOLDRegress-LFP and the corresponding time-lag location was determined. Furthermore, one standard deviation of the correlation mean at the maximum peak was calculated for each LFP.

3.6 Time-lag BOLD-LFP for All Scans - Dexmedetomidine

Time-lag BOLD-LFP correlation results were different for dexmedetomidine (Fig. 3.6) compared to isoflurane. First, dexmedetomidine BOLD-LFP time-lag correlations for higher frequencies were overall weaker. Maximum correlation was 0.14 for r-BOLD-Infraslow (Tab. 3.2). Time-lag for infraslow, delta, and theta peak correlation ranged between 1.5 and 3.5 seconds (Fig. 3.2). After QPP regression, greatest BOLD correlation change occurred at r-BOLD-Infraslow with a decrease of 0.09 at maximum peak (Tab. 3.2). When excluding infraslow LFP results, maximum correlation ranged between 0.01 and 0.07. Smaller correlation differences were shown after QPP regression for alpha, beta, and gamma frequencies. Despite overall smaller correlation changes, dexmedetomidine results still showed that QPP regression decreases BOLD-LFP correlation. As mentioned before, the plots were calculated using the left electrode as seed signal.

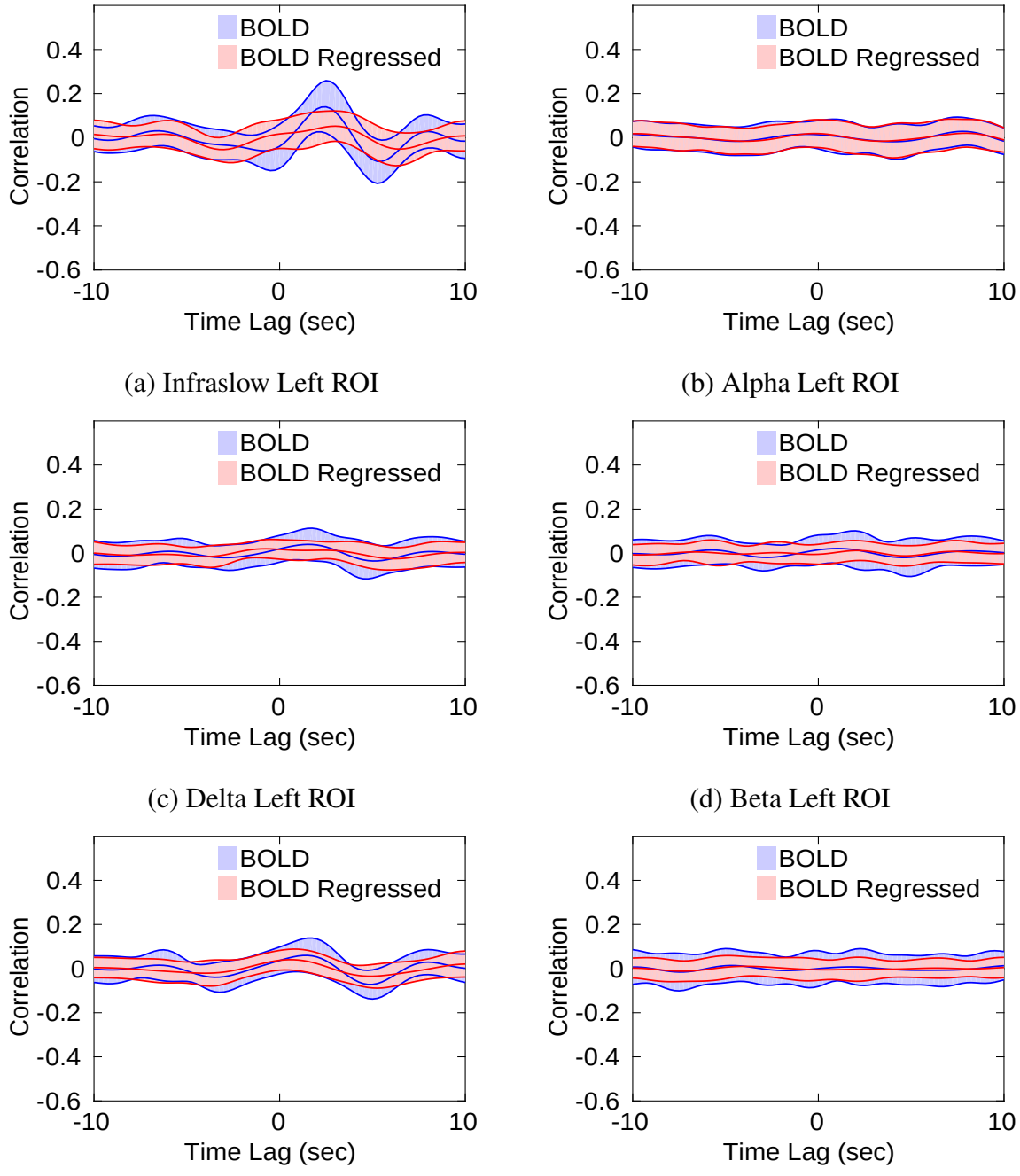

(a) Infraslow Left ROI

(b) Alpha Left ROI

(c) Delta Left ROI

(d) Beta Left ROI

(e) Theta Left ROI

(f) Gamma Left ROI

Figure 3.6: Time-lag correlation left ROI - dexmedetomidine. Figures illustrate time-lag cross correlations of the left S1FL region before (Blue) and after (Red) QPP regression for all rats and scans under dexmedetomidine conditions. Positive time-lag indicates LFP preceded BOLD signal. The plot illustrates mean (middle line) and one standard deviation (shaded region) of correlation for all scans using dexmedetomidine. The correlation scale ranges between 0.6 and -0.6. The time-lag ranges between -10 and 10 seconds.

Table 3.2: Time-lag maximum correlation results of the left S1FL - dexmedetomidine.

	BOLD Before QPP		BOLD After QPP		BOLD Corr Diff	
LFP	Time-lag (sec)	Peak Correlation	Time-lag (sec)	Peak Correlation	Time-lag (sec)	Peak Correlation
Infraslow	2.5	0.14 ± 0.12	3.0	0.05 ± 0.07	2.3	0.09 ± 0.13
Delta	1.5	0.04 ± 0.07	-0.8	0.02 ± 0.04	1.5	0.03 ± 0.07
Theta	1.5	0.06 ± 0.08	0.5	0.04 ± 0.05	7.8	0.03 ± 0.06
Alpha	-10.0	0.02 ± 0.06	2.5	0.01 ± 0.05	-10	0.02 ± 0.05
Beta	1.0	0.02 ± 0.07	2.0	0.01 ± 0.05	0.3	0.02 ± 0.06
Gamma	-4.8	0.01 ± 0.08	-4.0	0.01 ± 0.05	1.5	0.01 ± 0.06

This table is based on results shown in Figure 3.6. Maximum mean time-lag correlation (Max r-BOLD-LFP) was calculated, and time-lag location (Time-Lag (Sec)) of the maximum correlation was determined for each LFP band within the left S1FL region. Maximum time-lag correlation and the corresponding time-lag location for BOLD regressed (r-BOLDRegress-LFP) was calculated. Lastly, the maximum difference in correlation between r-BOLD-LFP and r-BOLDRegress-LFP and the corresponding time-lag location was determined. Furthermore, one standard deviation of the correlation mean at the maximum peak was calculated for each LFP.

3.7 Histogram - Time-Lag Maximum Correlation - Isoflurane

Maximum correlation values were analyzed to determine statistical significance before and after QPP regression for all LFP frequency bands under isoflurane anesthesia. Using maximum correlation values from positive time-lags (Fig. 3.5), histograms were plotted as a function of maximum correlation difference for each scan (Fig. 3.7) under isoflurane conditions. 17 scans were used to create the histogram for each LFP band. A one-sided paired t-test with a significance level of 0.01 was used to determine statistical differences between peak correlation BOLD (max r-BOLD-LFP) and BOLD regressed correlations (max r-BOLDRegress-LFP). Statistical significance was observed for infraslow and all higher LFP frequencies.

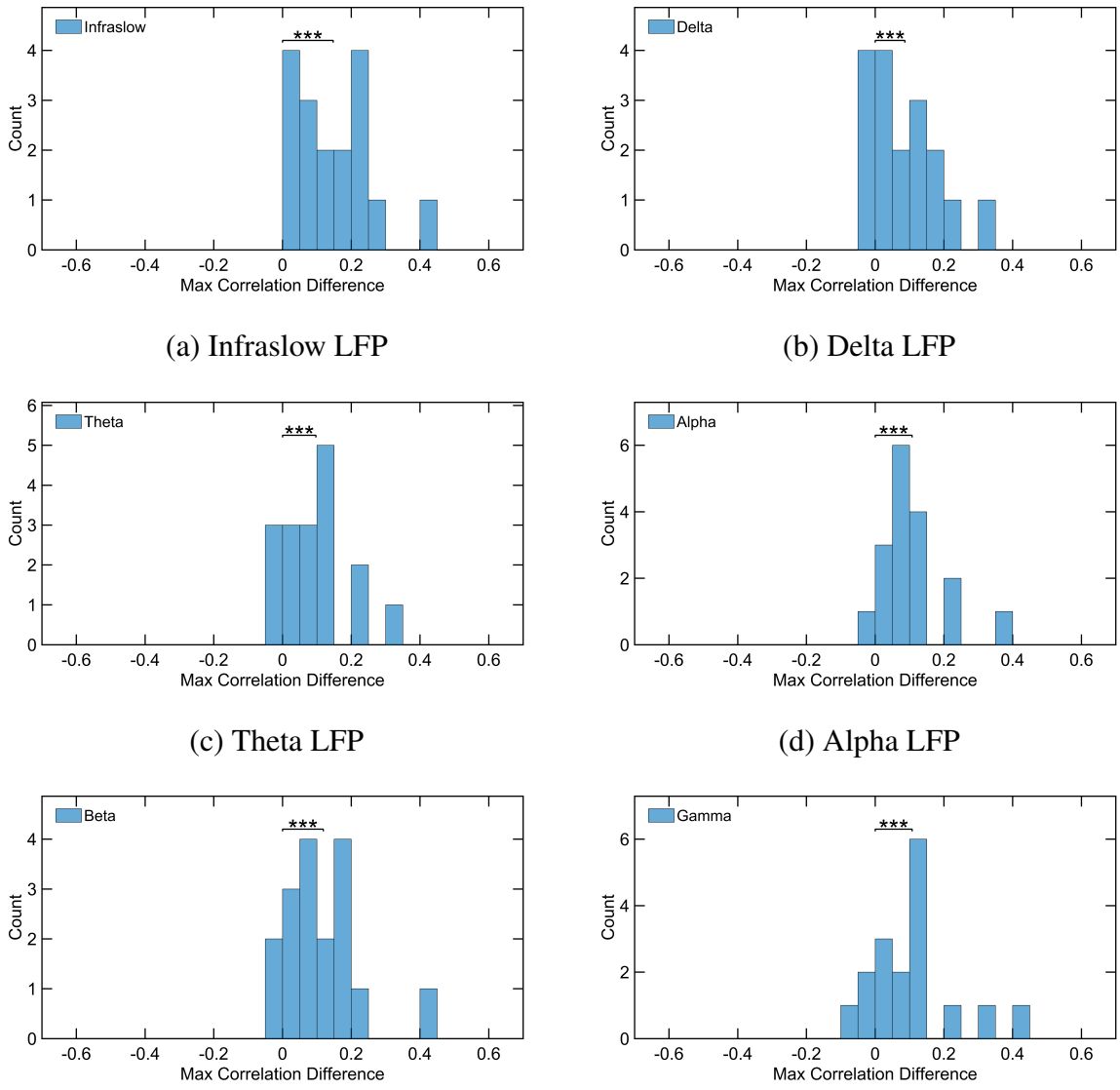

(a) Infraslow LFP

(b) Delta LFP

(c) Theta LFP

(d) Alpha LFP

(e) Beta LFP

(f) Gamma LFP

Figure 3.7: Histogram of time-lag maximum correlation with isoflurane for multiple LFP bands. The histogram displays maximum correlation changes before and after QPP regression for each scan at multiple LFP frequency bands under isoflurane anesthesia. Correlation bins have a width of 0.05. *** indicates statistical significance at the 0.01 level. (a) Maximum correlation difference at infraslow LFP shows statistically significance ($t(15) = 5.5084, p < 2.3834 \times 10^{-5}$) (b) Maximum correlation difference at delta LFP shows statistically significance ($t(15) = 3.8692, p < 6.7962 \times 10^{-4}$) (c) Maximum correlation difference at theta LFP shows statistically significance ($t(15) = 4.1897, p < 3.4667 \times 10^{-4}$) (d)Maximum correlation difference at alpha LFP shows statistically significance ($t(15) = 4.4847 p < 1.8761 \times 10^{-4}$) (e) Maximum correlation difference at beta LFP shows statistically significance ($t(15) = 4.5990 p < 1.4819 \times 10^{-4}$) (e) Maximum correlation difference at gamma LFP shows statistically significance ($t(15) = 3.7946 p < 7.9540 \times 10^{-4}$).

3.8 Histogram - Time-Lag Maximum Correlation - Dexmedetomidine

Similar histograms were plotted for dexmedetomidine conditions as shown previously with isoflurane anesthesia. Using maximum correlation values from positive time-lags (Fig. 3.6), histograms were plotted based on the maximum correlation difference before and after QPP regression for each scan under dexmedetomidine conditions (Fig. 3.8). 43 scans were used to create the histogram for each LFP band. A one-sided paired t-test with a significance level of 0.01 was used to determine statistical differences between peak correlation BOLD (max r-BOLD-LFP) and BOLD regressed correlations (max r-BOLDRegress-LFP). The paired t-test showed significance for infraslow and higher frequency LFP bands.

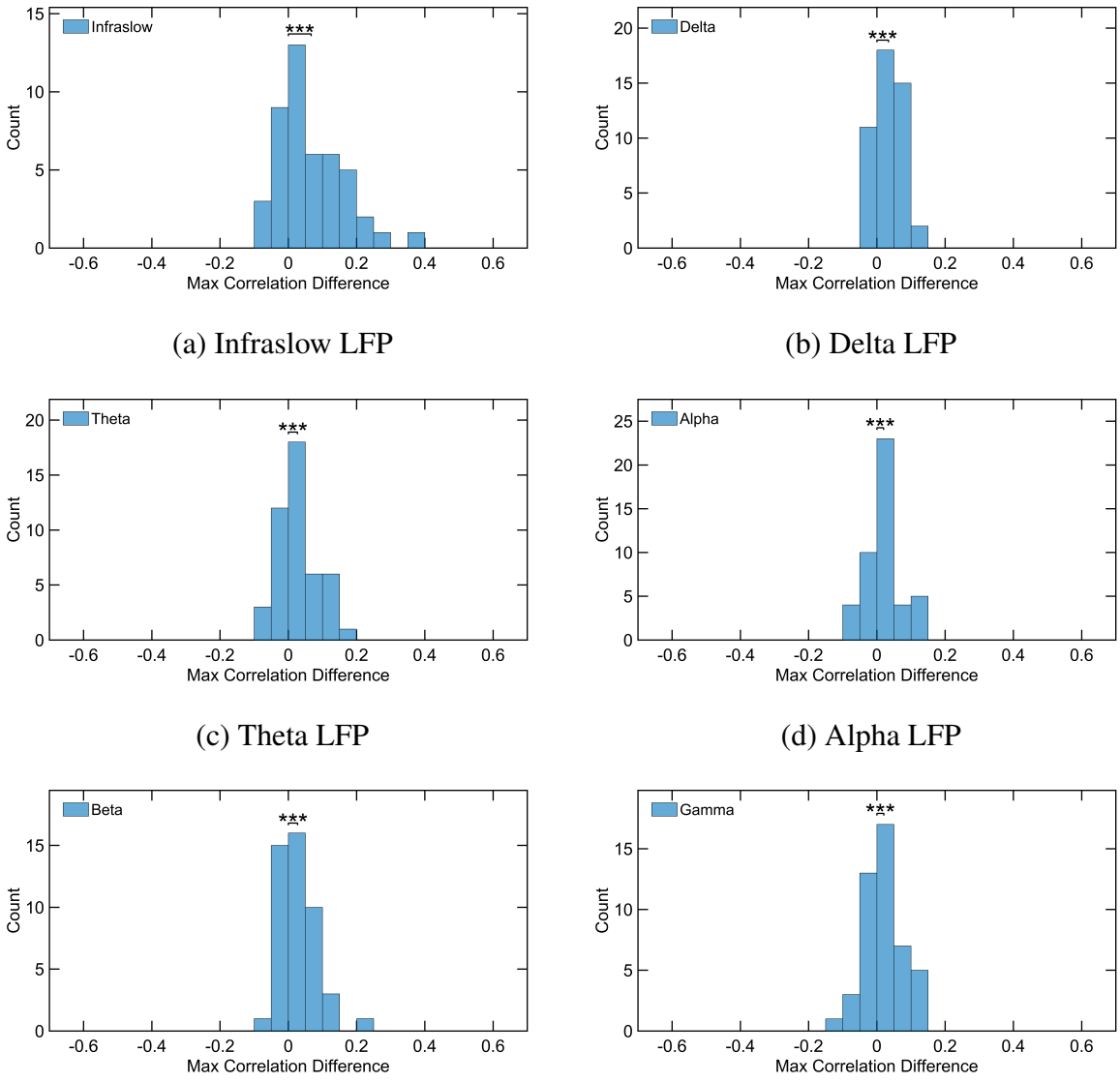

(a) Infraslow LFP

(b) Delta LFP

(c) Theta LFP

(d) Alpha LFP

(e) Beta LFP

(f) Gamma LFP

Figure 3.8: Histogram of time-lag maximum correlation with dexmedetomidine for multiple LFP bands. The histogram displays maximum correlation changes before and after QPP regression for each LFP frequency bands under dexmedetomidine anesthesia. Correlation bins have a width of 0.05. *** indicates statistical significance at the 0.01 level. (a) Maximum correlation difference at infraslow LFP shows statistically significance ($t(44) = 4.8760, p < 6.9433 \times 10^{-6}$) (b) Maximum correlation difference at delta LFP shows statistically significance ($t(44) = 5.4102, p < 1.1608 \times 10^{-6}$) (c) Maximum correlation difference at theta LFP shows statistically significance ($t(44) = 3.0193, p < 0.0021$) (d)Maximum correlation difference at alpha LFP shows statistically significance ($t(44) = 2.8105, p < 0.0036$) (e) Maximum correlation difference at beta LFP shows statistically significance ($t(44) = 3.3529, p < 8.1477 \times 10^{-4}$) (e) Maximum correlation difference at gamma LFP shows statistically significance ($t(44) = 2.4772, p < 0.0085$).

CHAPTER 4
DISCUSSION

This section will focus on three main topics: 1) BOLD correlation before QPP regression. 2) BOLD correlation after QPP regression. 3) QPP component based on the BOLD correlation difference before and after QPP regression.

4.1 BOLD correlation before QPP regression

Time-lag corresponding to peak correlation was found between 3.25 to 5 seconds for isoflurane and 1.5 to 3.5 seconds for dexmedetomidine. As mentioned before, positive time-lags illustrate BOLD signal lagging behind LFP data. Based on time-lag ranges, peak positive correlation time-lag most likely represents the hemodynamic response. These time lags align with previous studies that analyzed time-lag correlation between BOLD and electrophysiology [3, 14]. Shorter time-lag for dexmedetomidine compared to isoflurane may be explained by different empirical filters. Differences in empirical filter between isoflurane and dexmedetomidine most likely reflect vascular effects from each anesthesia. Isoflurane induces vasodilation by blocking potassium-ATP channels in smooth muscle [22] whereas dexmedetomidine influences alpha receptors that bind to smooth muscle and induce vasoconstriction [23]. Differences in the empirical filter from vascular effects most likely played a factor in different peak time-lags [18].

Infraslow correlation demonstrated greater peak correlation than higher BLP frequencies. For isoflurane, the strongest BOLD correlation of 0.21 was observed with infraslow LFP. Unlike expectation, strong correlations were also observed with all higher BLP frequencies except for delta band. One possible explanation for the strong correlations may be explained by the burst suppression pattern that is commonly observed with high isoflurane

levels. LFP alternates between bursting state and non-bursting state under high isoflurane levels [24]. Alternation of low and high frequency neural activity at similar time points may have caused both infraslow and higher BLP frequencies to have similar fluctuation patterns. One way to confirm this explanation would be analyzing rat data with lower isoflurane concentrations and see if BOLD correlation still maintains strong correlation for both infraslow and higher BLP. A study by Pan et al. showed an increase in isoflurane level decreases higher frequency LFP power coherence and increases lower frequency BOLD coherence [3] which aligns with results shown in this study. Another possible reason for strong high frequency correlation may be explained by a high degree of synchronization between infraslow and higher BLP frequencies. One study used EEG to find infraslow signals to be synchronized with higher frequencies in humans under sleeping conditions [16].

For dexmedetomidine anesthesia, infraslow BOLD signal exhibited the strongest correlation with infraslow LFP. Only delta and theta BLP showed a distinct peak in the time-lag correlation plot (Fig. 3.6) whereas alpha, beta, and gamma BLP did not have a distinguishable correlation peak. The overall correlation values under dexmedetomidine were smaller compared to isoflurane and may be linked to the different anesthetic mechanism. Another possible reason may be the decrease in power with increasing frequency (inverse relationship of power and frequency). A larger dataset for dexmedetomidine may help with improving power estimation.

4.2 BOLD after QPP regression and LFP

The time-lag at peak correlation after QPP regression showed more variability but still captured the hemodynamic response. Time-lag ranged between 3.3 and 5.3 seconds for isoflurane and 0.5 to 3 seconds for dexmedetomidine. The time-lags lie within the hemodynamic response. As mentioned before, the different anesthesia vascular effects may explain the

differences in time-lag. Even after QPP regression, the BOLD correlation seems to capture the hemodynamic response.

The peak correlation values after QPP regression were very small and hard to interpret. The peak correlation values ranged between 0.03 to 0.07 for isoflurane and 0.01 to 0.05 for dexmedetomidine. For isoflurane, the alpha peak correlation of 0.07 was the strongest compared to infraslow frequency band. For dexmedetomidine, infraslow peak correlation of 0.05 was only slightly higher than alpha correlation of 0.04. Larger differences between infraslow and higher BLP correlations were not observed after BOLD QPP regression. This shows that BOLD correlation after QPP regression is less linked to infraslow frequencies and more linked to higher frequencies. However, this argument is difficult to make because of the small correlation values. Future studies on awake rats may reveal more differences between the different frequency bands with BOLD after QPP regression because the rats won't be affected by specific anesthesia effects.

4.3 QPP Component (Difference in BOLD before and after QPP regression)

The correlation difference between BOLD before and after QPP regression revealed information about the QPP component. Greatest correlation difference was observed with infraslow BOLD correlation for both isoflurane and dexmedetomidine anesthesia. Correlation differences were shown for all higher frequencies but lesser degree compared to infraslow. Clearly, QPP components are an important aspect of spatiotemporal patterns of the BOLD signal. One possible interpretation of this result is that quasi-periodic patterns (QPP) found in infraslow BOLD is influenced by all frequencies. A similar study done by Thompson et al. [21] demonstrated that QPP correlated to infraslow LFP but QPP only correlated to high frequency (25-40Hz or high beta) BLP for isoflurane. Those results align with this study where greatest difference in BOLD correlation before and after QPP regression was found in infraslow LFP for both isoflurane and dexmedetomidine. Unlike

Thompson et al. where only one high frequency band was compared, this study compared BOLD correlation with multiple higher frequency LFP bands. A study by Hughes et al. demonstrated infraslow oscillations are linked to changes in alpha band (8-13Hz) within the thalamic region with cats [25]. Furthermore, there has been more evidence showing cross-frequency coupling as a method for the brain to transfer information at various distances using high and low frequency oscillations [26]. This study provides more evidence that infraslow and higher frequency neural activities contribute to large-scale networks observed through quasi-periodic patterns. Future studies may be able to address whether infraslow frequency directly affects higher frequencies or higher frequencies modulate infraslow frequencies.

4.4 Clinical Potential

BOLD and QPP may provide valuable information to assist in clinical diagnosis and spatial mapping. More studies have shown the use of resting-state fMRI to distinguish healthy patients from people with a neurological disorder such as schizophrenia [8] and cognitive disorders [17]. A preliminary study in our lab utilized quasi-periodic patterns to show a larger contribution of QPPs to functional connectivity for people with major depressive disorders [27]. Regression of QPP from BOLD may provide another avenue for diagnosing different disorders. Furthermore, QPP can provide high spatial resolution to map the infraslow electrical activity of an entire brain compared to EEG that provide lower resolution surface level electrical information.

4.5 Limitation

Although BOLD signals reflect neural activity, there have been studies showing that BOLD signals can be influenced by non-neural activity. Vasomotion and respiration have been shown to change BOLD signals [28]. Imaging system noise and MRI artifacts affect BOLD signals [29]. Furthermore, level of arousal contributes to changes in functional connectiv-

ity [30]. Careful experimental setup in this study helped minimize effects from these non-neural based origins such as reducing motion with a head holder or maintaining anesthesia levels [13, 12]. However, the BOLD signal in this study may contain a mixture of neural and non-neural processes despite attempts to reduce non-neural influences. Investigating microscopic level of metabolism or measuring calcium concentrations would provide additional information to help distinguish neural and non-neural contributions of the BOLD signal within these studies.

Another limitation of this study is the lack of statistical power. Only a total of ten rats were utilized in this study for both anesthesia conditions which is reflected in the high standard deviation correlations plots (Tab. 3.1 and 3.2). Furthermore, some rats were scanned more often up to 15 scans and other rats were scanned less than five times. Due to the lack of experimental data, all the rat scans were combined to produce the results. In future studies, an analysis of the scans within each rat would provide a better understanding of QPP and BOLD signals.

CHAPTER 5
CONCLUSION

This study was able to examine the effects of QPP regression on BOLD correlation in relation to infraslow and higher LFP frequencies. The results after QPP regression were unclear due to very small correlation values but seem to suggest that BOLD signal is driven less by infraslow and more from higher frequency neural activity. The greatest change in correlation occurred in the infraslow band for isoflurane and dexmedetomidine anesthesia, which confirms QPP reflect a large portion of the spontaneous spatiotemporal BOLD signal. Results also suggest that higher LFP frequencies do play a role in QPP but to a lesser degree depending on the anesthesia. The study shows the importance of analyzing both infraslow and higher LFP frequencies in relation to BOLD and QPP.

REFERENCES

[1] W Majeed, M Magnuson, and S. Keilholz, "Spatiotemporal dynamics of low frequency fluctuations in bold fmri of the rat," *Journal of Magnetic Resonance Imaging*, vol. 30, no. 2, pp. 384–393, 2009.

[2] G. Thompson, W. Pan, M. Magnuson, D Jaeger, and S. Keilholz, "Quasi-periodic patterns (qpp): Large-scale dynamics in resting state fmri that correlate with local infraslow electrical activity," *Neuroimage*, vol. 84, pp. 1018–1031, 2014.

[3] W.-J. Pan, G. Thompson, M. Magnuson, W. Majeed, D. Jaeger, and S. Keilholz, "Broadband local field potentials correlate with spontaneous fluctuations in functional magnetic resonance imaging signals in the rat somatosensory cortex under isoflurane anesthesia," *Brain Connectivity*, vol. 1, no. 2, 119131, 2011.

[4] S. Ogawa, R. S. Menon, D. W. Tank, S. G. Kim, H. Merkle, J. M. Ellermann, and K. Ugurbil, "Functional brain mapping by blood oxygenation level-dependent contrast magnetic resonance imaging. a comparison of signal characteristics with a biophysical model," *Biophysical Journal*, vol. 64, no. 3, 803812, 1993.

[5] B. Biswal, F. Zerrin Yetkin, V. M. Haughton, and J. S. Hyde, "Functional connectivity in the motor cortex of resting human brain using echo-planar mri," *Magnetic Resonance in Medicine*, vol. 34, no. 4, pp. 537–541, 1995.

[6] M. Raichle, A. MacLeod, A. Snyder, W. Powers, D. Gusnard, and G. Shulman, "A default mode of brain function," *Proc Natl Acad Sci U S A.*, vol. 98, no. 2, pp. 676–82, 2001.

[7] M. D. Fox, A. Z. Snyder, J. L. Vincent, M. Corbetta, D. C. Van Essen, and M. E. Raichle, "The human brain is intrinsically organized into dynamic, anticorrelated functional networks," *Proceedings of the National Academy of Sciences of the United States of America*, vol. 102, no. 27, pp. 9673–9678, 2005.

[8] U Sakoglu, G. Pearlson, K. Kiehl, Y. Wang, A. Michael, and V. Calhoun, "A method for evaluating dynamic functional network connectivity and task-modulation: Application to schizophrenia.," *MAGMA*, vol. 23, no. 5-6, pp. 351–66, 2010.

[9] V. Calhoun, R. Miller, G. Pearlson, and T. Adal, "The chronnectome: Time-varying connectivity networks as the next frontier in fmri data discovery," *Neuron*, vol. 84, no. 2, pp. 262 –274, 2014.

[10] W Majeed, M Magnuson, W Hasenkamp, H Schwarb, E. Schumacher, L Barsalou, and S. Keilholz, "Spatiotemporal dynamics of low frequency bold fluctuations in rats and humans," *Neuroimage*, vol. 54, no. 2, pp. 1140–1150, 2011.

[11] A Shumuel and D. Leopold, "Neuronal correlates of spontaneous fluctuations in fmri signals in monkey visual cortex: Implications for functional connectivity at rest," *Human Brain Mapping*, vol. 29, no. 7, pp. 751–761, 2008.

[12] W. Pan, G. Thompson, M. Magnuson, W. Majeed, D. Jaeger, and S. Keilholz, "Simultaneous fmri and electrophysiology in the rodent brain.," *J. Vis. Exp.*, vol. 42, e1901, 2010.

[13] W. Pan, G. Thompson, M. Magnuson, D Jaeger, and S Keilholz, "Infraslow lfp correlates to resting-state fmri bold signals," *Neuroimage*, vol. 74, pp. 288–297, 2013.

[14] G. Thompson, M. Merritt, W. Pan, M. Magnuson, J. Grooms, D Jaeger, and S. Keilholz, "Neural correlates of time-varying functional connectivity in the rat," *Neuroimage*, vol. 83, pp. 826–836, 2013.

[15] S. Kannurpatti, B. Biswal, Y. Kim, and B. Rosen, "Spatio-temporal characteristics of low-frequency bold signal fluctuations in isoflurane-anesthetized rat brain," *Neuroimage*, vol. 40, no. 4, pp. 1738–1747, 2008.

[16] S. Vanhatalo, J. M. Palva, M. D. Holmes, J. W. Miller, J. Voipio, and K. Kaila, "Infraslow oscillations modulate excitability and interictal epileptic activity in the human cortex during sleep," *Proceedings of the National Academy of Sciences of the United States of America*, vol. 101, no. 14, pp. 5053–5057, 2004. eprint: `http://www.pnas.org/content/101/14/5053.full.pdf`.

[17] J. Chen, X. Duan, H. Shu, Z. Wang, Z. Long, D. Liu, W. Liao, Y. Shi, H. Chen, and Z. Zhang, "Differential contributions of subregions of medial temporal lobe to memory system in amnestic mild cognitive impairment: Insights from fmri study," *Scientific reports*, vol. 6, srep26148, 2016.

[18] D. Aksenov, L. Li, M. Miller, G Iordanescu, and A. Wyrwicz, "Effects of anesthesia on bold signal and neuronal activity in the somatosensory cortex," *Journal of Cerebral Blood Flow and Metabolism*, vol. 35, no. 11, pp. 1819–1826, 2015.

[19] X. Liu, X.-H. Zhu, Y. Zhang, and W. Chen, "Neural origin of spontaneous hemodynamic fluctuations in rats under burstsuppression anesthesia condition. cerebral cortex," *Cerebral Cortex*, vol. 21, pp. 374–384, 2011.

[20] M. E. Magnuson, G. J. Thompson, W.-J. Pan, and S. D. Keilholz, "Time-dependent effects of isoflurane and dexmedetomidine on functional connectivity, spectral char-

acteristics, and spatial distribution of spontaneous bold fluctuations," *NMR in biomedicine*, vol. 27, no. 3, pp. 291–303, 2014.

[21] W. Thompson GJ Pan and S. Keilholz, "Different dynamic resting state fmri patterns are linked to different frequencies of neural activity," *Biophysical Journal*, vol. 114, no. 1, pp. 114–24, 2015.

[22] D. A. Schwinn, R. W. McIntyre, and J. Reves, "Isoflurane-induced vasodilation: Role of the [alpha]-adrenergic nervous system.," *Anesthesia & Analgesia*, vol. 71, no. 5, pp. 451–459, 1990.

[23] R. Gertler, H. C. Brown, D. H. Mitchell, and E. N. Silvius, "Dexmedetomidine: A novel sedative-analgesic agent," *Proceedings (Baylor University. Medical Center)*, vol. 14, no. 1, p. 13, 2001.

[24] J.-F. Ferron, D. Kroeger, O. Chever, and F. Amzica, "Cortical inhibition during burst suppression induced with isoflurane anesthesia," *Journal of Neuroscience*, vol. 29, no. 31, pp. 9850–9860, 2009. eprint: `http://www.jneurosci.org/content/29/31/9850.full.pdf`.

[25] S. W. Hughes, M. L. Lőrincz, H. R. Parri, and V. Crunelli, "Infra-slow (¡ 0.1 hz) oscillations in thalamic relay nuclei: Basic mechanisms and significance to health and disease states," *Progress in brain research*, vol. 193, p. 145, 2011.

[26] R. T. Canolty and R. T. Knight, "The functional role of cross-frequency coupling," *Trends in cognitive sciences*, vol. 14, no. 11, pp. 506–515, 2010.

[27] K. Wang, W. Majeed, G. Thompson, K. Ying, Y. Zhu, and S. Keilholz, "Quasi-periodic pattern of fmri contributes to functional connectivity and explores difference between major depressive disorder and control," in *International Society for ISMRM Magnetic Resonance in Medicine*, ser. 24th Annual Meeting and Exhibition 07-13, Singapore, 2016.

[28] K. Murphy, R. M. Birn, and P. A. Bandettini, "Resting-state fmri confounds and cleanup," *Neuroimage*, vol. 80, pp. 349–359, 2013.

[29] P. A. Bandettini, A Jesmanowicz, J. Van Kylen, R. M. Birn, and J. S. Hyde, "Functional mri of brain activation induced by scanner acoustic noise," *Magnetic resonance in medicine*, vol. 39, no. 3, pp. 410–416, 1998.

[30] E. Tagliazucchi and H. Laufs, "Decoding wakefulness levels from typical fmri resting-state data reveals reliable drifts between wakefulness and sleep," *Neuron*, vol. 82, no. 3, pp. 695–708, 2014.